Giant Optical Anisotropy in the UV-Transparent 2D Nonlinear Optical Material $Sc(IO_3)_2(NO_3)$

Chao Wu,[a],† Xingxing Jiang,[b],† Zujian Wang,[c],† Zheshuai Lin,[b] Zhipeng Huang,[a] Xifa Long,[c] Mark G. Humphrey,[d] and Chi Zhang*[a]

[a] Dr. C. Wu, Prof. Z. Huang, Prof. C. Zhang
China-Australia Joint Research Center for Functional Molecular Materials, School of Chemical Science and Engineering, Tongji University, Shanghai 200092, China
E-mail: chizhang@tongji.edu.cn
[b] Dr. X. Jiang, Prof. Z. Lin
Technical Institute of Physics and Chemistry, Chinese Academy of Sciences, Beijing 100190, China
[c] Dr. Z. Wang, Prof. X. Long
Key Laboratory of Optoelectronic Materials Chemistry and Physics, State Key Laboratory of Structure Chemistry, Fujian Institute of Research on the Structure of Matter, Chinese Academy of Sciences, Fuzhou, Fujian 350002, China
[d] Prof. M. G. Humphrey
Research School of Chemistry, Australian National University, Canberra, ACT 2601, Australia
[†] These authors contributed equally to this work

Supporting information for this article is given via a link at the end of the document.

Abstract: Birefringence is a fundamental optical property for linear and nonlinear optical (NLO) materials. Thus far, it has proved to be very difficult to engineer large birefringence in optical crystals functioning in the UV region. Herein, we report the first 2D rare-earth iodate-nitrate crystal $Sc(IO_3)_2(NO_3)$ (SINO), which is shown to exhibit giant optical anisotropy. Air-stable SINO possesses a short UV absorption edge (298 nm), a strong NLO response (4.0 times that of benchmark KH_2PO_4) for the nitrate family, and the largest birefringence (Δn = 0.348 at 546 nm) of inorganic oxide optical crystals. The unusually large birefringence and NLO response can be attributed to an optimized 2D layered structure, combined with highly polarizable and anisotropic building units $[IO_3]^-$ and $[NO_3]^-$. These findings will facilitate development of UV linear and NLO materials with giant optical anisotropy, and promote their potential applications in optoelectronic devices.

Linear optical birefringent and nonlinear optical (second-harmonic generation (SHG)) crystals have attracted considerable interest in many branches of science and technology, such as all-solid-state lasers, optical communications, and advanced instrumentation.[1,2] Birefringence, determined by optical anisotropy, is the most important and fundamental optical parameter for optical materials.[3] Large birefringence enables the efficient manipulation of light propagation, permitting modulation of the light polarization of birefringent materials and the phase-matchability of SHG crystals.[4-5] Ultraviolet (UV) (λ < 400 nm) light generated by optical crystal materials is indispensable in a rapidly increasing number of emerging applications for short-wavelength light sources in fields such as semiconductor lithography, precision manufacturing, and biological gene engineering.[6] However, a short UV absorption edge (corresponding to a wide band gap) is usually inversely proportional to large birefringence.[7] For example, commercialized YVO_4[8a] and calcite $(CaCO_3)$[8b] possess large birefringence, but they can only be used in the visible or near-infrared regions because of their low transmittance in the UV region. The NLO crystal SrB_4O_7[9] has a short UV absorption edge, but its small birefringence renders conventional phase-matching impossible in SHG. As a result, the pursuit of suitable UV optical materials with large birefringence remains a major challenge in contemporary materials research.

Inorganic π-conjugated systems, including borates, carbonates, and nitrates, have been of long-standing interest in the quest for UV optical crystals because their strong covalent bonds may induce short absorption edges.[10] Unfortunately, the birefringence coefficients of most inorganic π-conjugated materials are not demonstrably superior to those of traditional oxides such as vanadates, tellurotungstates, or telluromolybdates.[8a,11] Several strategies have been developed to enhance or optimize the birefringence of π-conjugated materials: (a) Condensation of π-conjugated $[BO_3]^{3-}$ groups, examples including $Li_2Na_2B_2O_5$[12a] and CaB_2O_4.[12b] (b) Incorporation of fluorinated tetrahedral anions such as $[BO_xF_{4-x}]^{(x+1)-}$, which has led to a series of deep-UV fluorooxoborates $M_2B_{10}O_{14}F_6$ (M = Ca, Sr),[13a] CsB_4O_6F,[13b] and $SrB_5O_7F_3$[13c] with enhanced birefringence. (c) Introduction of second-order Jahn-Teller (SOJT) cations, such as d^0 transition metal (TM) cations (e.g., V^{5+}, Nb^{5+}) and lone-pair cations (e.g. Pb^{2+}, Sn^{2+}, Sb^{3+}, etc.); relevant examples include SbB_3O_6,[14a] $Sn_2B_5O_9Cl$,[14b] and $Pb_2(NO_3)_2(H_2O)F_2$.[14c] The approaches to date have mainly focused on the combination of metal cation and single oxyanion; the combination of two types of oxyanions into the one structure to create new UV NLO materials with large birefringence is thus far underexploited because of the intricate multiple inter-anion interactions.

In principle, birefringence is intimately related to the anisotropic structure building units (SBUs) and their spatial arrangement in the crystal structure. Of the possible crystalline arrangements, one can achieve large anisotropy in 2D materials in which anisotropic SBUs are arranged in parallel layer-like structures.[10j] In the present work, we propose to introduce I^{5+}-centered $[IO_3]^-$ oxyanions[15] into a π-conjugated system to create a 2D layered structure with large birefringence in the UV region. Unlike π-conjugated anions, the lone-pairs of the $[IO_3]^-$ oxyanion[16] usually exhibit large optical anisotropy and polarizability when they are properly aligned; this favors generation of large birefringence and SHG responses. In comparison with structures containing only a single π-conjugated oxyanion,[17] 2D layered structures with two different

anisotropic SBUs may possess additive polarizability anisotropy due to differences between their intralayer bonding and interlayer interaction. We report herein the first example of a 2D NLO crystal, the rare-earth iodate-nitrate $Sc(IO_3)_2(NO_3)$ (SINO), via a homovalent oxyanion substitution of the parent $Sc(NO_3)_3$. SINO has a short UV absorption edge of 298 nm, a very strong SHG response (4.0 × KH_2PO_4 (KDP)), and the largest birefringence (Δn = 0.348 at 546 nm) of any inorganic oxide optical crystal. This homovalent oxyanion substitution strategy may provide a new modus for the development of UV optical materials with large birefringence.

Colorless transparent block crystals of SINO (Figure S1) were synthesized via hydrothermal methods at 160 ºC using $Sc(NO_3)_3{\cdot}6H_2O$, HIO_3 and nitric acid aqueous solution as starting materials. SINO crystals are nonhygroscopic, remaining transparent without any change in weight or visible appearance after three-months exposure to air at room temperature.

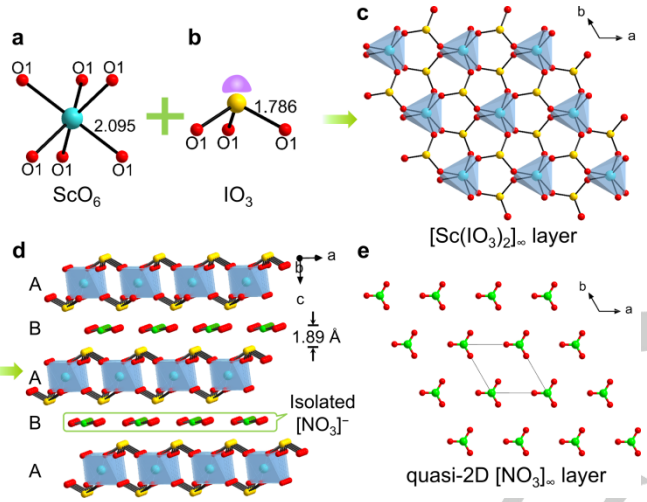

Figure 1. (a) Regular [ScO_6] octahedron. (b) [IO_3] trigonal pyramid. (c) $[Sc(IO_3)_2]_\infty$ layer in the *ab* plane. (d) Crystal structure of $Sc(IO_3)_2(NO_3)$. (e) quasi-2D $[NO_3]_\infty$ layer in the *ab* plane.

SINO crystallizes in the non-centrosymmetric (NCS) trigonal space group *R*32 (No. 155) (Tables S1 and S2). Its crystal structure is composed of honeycomb-like $[Sc(IO_3)_2]_\infty$ layers and quasi-2D $[NO_3]_\infty$ layers stacking in an -ABAB- sequence. Each Sc^{3+} cation is coordinated to six O1 atoms, forming a regular [ScO_6] octahedron with equal Sc−O bond distances of 2.096(10) Å (Figure 1a). Unlike lone-pair cations such as Pb^{2+} and Bi^{3+}, the rare-earth cation Sc^{3+} favors the transmission of short-wavelength UV light because of the absence of *d*-*d* and *f*-*f* electron transitions. The I^{5+} cation is bonded to three oxygen atoms, affording an [IO_3] trigonal pyramid with equal I-O bond lengths of 1.786(10) Å (Figure 1b). The six coordinated oxygen atoms in the [ScO_6] octahedra can be assigned to two distinct layers: three upper- and three lower-layer O1 atoms. Every [ScO_6] octahedron is linked to six [IO_3] trigonal pyramids by the O1 atoms, resulting in a honeycomb-like $[Sc(IO_3)_2]_\infty$ layer in the *ab* plane (Figure 1c). Notably, within each $[Sc(IO_3)_2]_\infty$ layer (Figure 1d), the upper- and lower-$[IO_3]_\infty$ layers adopt a face-to-face interplanar arrangement, while each $[IO_3]_\infty$ layer maintains a parallel alignment. The arrangement of the $[IO_3]^-$ groups of the honeycomb-like layers may favor superposition of the anisotropic polarizabilities, with potential for large birefringence.[18c] The N atoms are each bonded to three O atoms to form planar $[NO_3]$ triangles with equal N-O distances of 1.271(17) Å and O-N-O bond angles of 120.0° (Table S3). These isolated $[NO_3]^-$ groups adopt a coplanar aligned arrangement within the quasi-2D layers (Figures 1e and S2a), a favorable mode for generating large optical responses.

The most critical structural feature of SINO, however, is the spatial arrangement of the $[Sc(IO_3)_2]_\infty$ layers and quasi-2D $[NO_3]_\infty$ layers (interlayer spacing 1.89 Å: Figure 1d), which may greatly contribute to the unprecedented large birefringence of SINO. Firstly, the $[IO_3]^-$ groups inhibit the direct interactions between the rare-earth Sc^{3+} trications and the oxygen atoms of the $[NO_3]^-$ groups; this favors the formation of an anisotropic 2D layered structure. The $[NO_3]^-$ groups of the quasi-2D $[NO_3]_\infty$ layers therefore remain non-coordinated. The coplanar and parallel arrangement of the $[NO_3]^-$ groups contributes strongly to the linear and nonlinear optical properties.[18a] Secondly, based on the criteria identified by the Lezno group,[18b] $[IO_3]^-$ SBUs with their high polarizability anisotropies are introduced into a nitrate-containing structure. These $[IO_3]^-$ SBUs are also oriented with a mutually parallel alignment, controlled by the uniform alignment of the [ScO_6] octahedra (Figure S2b). Such an arrangement of the $[IO_3]^-$ groups is similar to that in the birefringent iodate $ZnIO_3F$ (Δn = 0.219).[18c] Clearly, the structure of SINO inherits the desirable layered arrangements of individual nitrates and iodates, suggesting that it may exhibit strong anisotropic linear optical activity. Thirdly, the alignment of the key optically-active $[NO_3]^-$ and $[IO_3]^-$ groups in the SINO crystal is optimal for additive polarizability anisotropy, as the $[Sc(IO_3)_2]_\infty$ layers and quasi-2D $[NO_3]_\infty$ layers are parallel to each other with a dihedral angle of 0° (Figure S2b), with significant differences between the interlayer interactions (originating from lone-pair containing oxyanions and π-conjugated oxyanions) and the intralayer bonding.

The UV-Vis-NIR diffuse reflectance spectrum indicates that SINO has a band gap of 4.15 eV, corresponding to an optical transparency window to 298 nm in the UV spectral region (Figure S3).

The birefringence of a SINO single crystal was measured on a ZEISS Axio A1 polarizing microscope. The SINO crystal can achieve complete extinction (Figures 2a and 2b). The measurement results showed that the retardation value of the

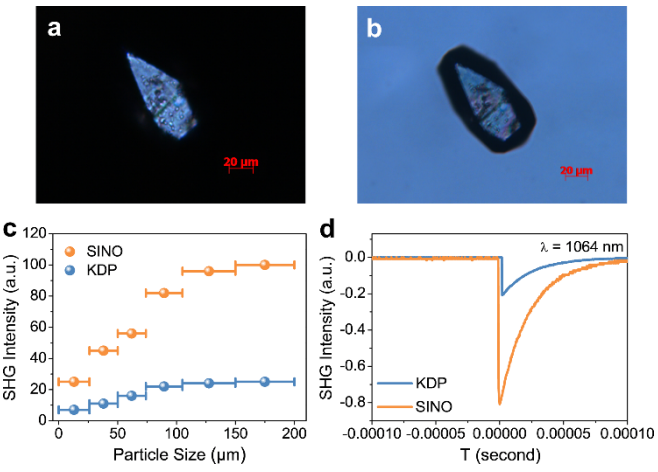

Figure 2. A comparison of (a) the original $Sc(IO_3)_2(NO_3)$ crystal and b) the $Sc(IO_3)_2(NO_3)$ crystal achieving complete extinction. (c) Phase-matching curves of $Sc(IO_3)_2(NO_3)$ and KDP with 1064 nm laser radiation. (d) Oscilloscope traces of the SHG signals (105−150 μm).

Table 1. Band gap and birefringence data for some representative inorganic oxide optical crystals.

Crystals	Birefringence	Band gap (eV)	Refs
α-BaB_2O_4	0.122 @589 nm$^{Exp.}$	6.56	19a
$Ba_2Ca(B_3O_6)_2$	0.1241 @589.3 nm$^{Exp.}$	6.97	19b
$Li_2Na_2B_2O_5$	0.095 @532 nm$^{Exp.}$	6.85	12a
$Sn_2B_5O_9Cl$	0.168 @546 nm$^{Exp.}$	3.53	14b
SbB_3O_6	0.290 @546 nm$^{Exp.}$	3.95	14a
YVO_4	0.226 @590 nm$^{Exp.}$	3.10	8a
$CaCO_3$	0.172 @589 nm$^{Exp.}$	5.90	8b
$KTiOPO_4$	0.106 @589 nm$^{Exp.}$	3.54	19c
$K_2Sb(P_2O_7)F$	0.157 @546 nm$^{Exp.}$	4.74	19d
$Cs_2TeMo_3O_{12}$	0.2039 @480 nm$^{Exp.}$	2.88	19e
$Na_2TeW_2O_9$	0.2069 @450 nm$^{Exp.}$	3.47	19f
$Bi(IO_3)F_2$	0.209 @1064 nm$^{Cal.}$	3.97	16
$ZnIO_3F$	0.219 @546 nm$^{Exp.}$	4.20	18c
$Pb_2(NO_3)_2(H_2O)F_2$	0.230 @1064 nm$^{Cal.}$	4.13	14c
$Sc(IO_3)_2(NO_3)$	0.348 @546 nm$^{Exp.}$	4.15	This work

measured crystal was approximately 18.39 μm with a thickness of 52.8 μm (Figure S4), corresponding to a measured birefringence of 0.348 at the wavelength of 546 nm (Supporting Information, Eqn. (1)) (Table 1). To the best of our knowledge, the birefringence of SINO is the largest value for inorganic oxide optical crystals.

As SINO crystallizes in an NCS space group, powder SHG measurements with laser radiation of 1064 nm were conducted using a KDP sample as a reference. As shown in Figure 2c, the SHG intensities depend linearly on the particle size, which suggests that SINO is phase-matchable at 1064 nm. SINO exhibits strong SHG signals that are about 4.0 times larger than that of KDP to 1064 nm laser radiation (particle diameter range 105−150 μm). This SHG performance is superior to those of other hetero-oxyanion nitrate NLO materials, such as $PbCdF(SeO_3)(NO_3)$ (2.6 × KDP),[20a] $Bi_3TeO_6OH(NO_3)_2$ (3.0 × KDP),[10i] $La(IO_3)_2(NO_3)$ (0.6 × KDP),[20b] $[LaPb_8O(OH)_{10}(H_2O)](NO_3)_7$ (1.3 × KDP),[20d] $Pb_2(SeO_3)(NO_3)_2$ (2.0 × KDP),[20e] and $Bi_2Te_2O_6(NO_3)_2(OH)_2(H_2O)$ (0.5 × KDP),[20c] being surpassed only by $Pb_2(BO_3)(NO_3)$ (9.0 × KDP).[10e]

Density functional theory calculations were performed to explore the origins of the excellent optical properties of SINO, including its strong SHG response and particularly large birefringence.[21] The calculated band structure (Figure S5) shows that SINO exhibits an indirect band gap of 2.51 eV, which is smaller than the experimental value because of the discontinuity of exchange correlation energy. According to the density of states and partial density of states projected onto the constituent atoms (Figure S6), N-2p, I-2p, O-2p and Sc-3d states form the bottom of the conduction band (CB), while O-2p, I-5p and Sc-3d states form the top of the valence band, which is consistent with $[ScO_6]^{9-}$, $[NO_3]^-$ and $[IO_3]^-$ units synergistically contributing to the excellent birefringence and SHG properties.

A more detailed study of the calculated refractive index dispersion and SHG performance was then undertaken. The refractive index dispersion curve reveals strong optical anisotropy and that SINO is a negative uniaxial crystalline material with $n_o > n_e$ in the low frequency range (Figure 3a). The derived birefringence (Δn) at 546 nm is 0.366, in good agreement with the experimental value. This large birefringence ensures that SINO can achieve good phase-matching across its entire transparency region and down to 298 nm. The SHG coefficient d_{ij} was calculated by the method of Lin et al.[22] SINO crystallizes in the *R*32 space group, with one non-zero independent SHG coefficient ($d_{11} = d_{22}$) under the restriction of Kleinman symmetry.[23] The calculated SHG tensors are $d_{11} = d_{22}$ = 1.49 pm V^{-1}, which is consistent with the experimental result (4.0 times that of KDP). The SHG-weighted electron density (Figures 3b and 3c) reveals that the occupied and unoccupied states are mainly contributed by $[NO_3]^-$ units, while the $[IO_3]^-$ units contribute only slightly to the SHG-weighted density.

To understand the specific optical contributions from the constituent units, a real-space atom-cutting method[24] was performed on SINO (Table S4). Both the 2D $[Sc(IO_3)_2]_\infty$ layers (constructed from the $[ScO_6]^{9-}$ and $[IO_3]^-$ groups) and the quasi-2D $[NO_3]_\infty$ layers exhibit large optical anisotropy. Specifically, the contribution from the $[Sc(IO_3)_2]^-$ units is 0.290, which is much larger than that of the $[NO_3]^-$ groups (0.121); the $[IO_3]^-$ groups in the 2D $[Sc(IO_3)_2]_\infty$ layer account for the majority of the birefringence. From the above analysis, it can be concluded that the $[Sc(IO_3)_2]^-$ and $[NO_3]^-$ units and their ordered arrangement in the optimized 2D layered structure all contribute to the strong anisotropic linear optical properties of SINO, and the $[NO_3]^-$ units make the dominant contributions to the SHG coefficients. Overall, the excellent performance for laser frequency conversion of SINO is attributed to a cooperative effect of the $[IO_3]^-$ and $[NO_3]^-$ units within the 2D layered structure.

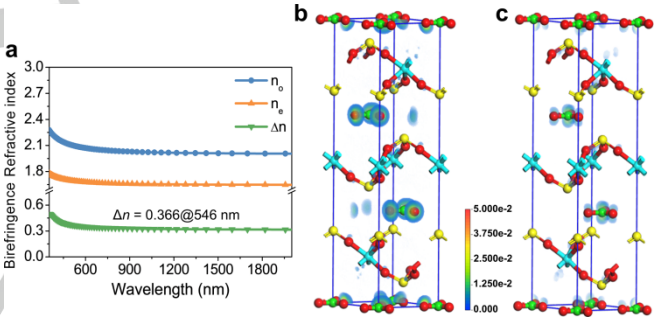

Figure 3. (a) Calculated refractive indices and birefringence of $Sc(IO_3)_2(NO_3)$. SHG-weighted density for (b) occupied and (c) unoccupied states in the virtual electron process.

In summary, the first 2D rare-earth iodate-nitrate $Sc(IO_3)_2(NO_3)$ has been prepared, featuring a giant optical anisotropy. This anisotropy arises from the optimal 2D layered structure of SINO, coupled with a judicious composition of the constituent units $[Sc(IO_3)_2]^-$ and $[NO_3]^-$. SINO not only possesses a large SHG response (4 × KDP) and a short UV absorption edge (298 nm), but also exhibits the largest birefringence ever reported for an inorganic oxide optical crystal (0.348 at 546 nm). These findings imply that SINO is an excellent UV transparent bi-functional optical material for both SHG and birefringence. Moreover, this design strategy for creating 2D layered structures with two types of oxyanions may afford a reliable and versatile structure-driven approach to novel optoelectronic functional materials.

Acknowledgements

This research was financially supported by the National Natural Science Foundation of China (no. 51432006), the Ministry of Education of China for the Changjiang Innovation Research Team (no. IRT14R23), the Ministry of Education and the State Administration of Foreign Experts Affairs for the 111 Project (no. B13025), and the Innovation Program of Shanghai Municipal Education Commission. C.W. thanks the National and Shanghai Postdoctoral Program for Innovative Talents (nos. BX201800216 and 2018192). M.G.H. thanks the Australian Research Council for support (DP170100411).

Keywords: hetero-oxyanion • 2D structure • ultraviolet • nonlinear optical materials • birefringent materials

[1] a) S. Y. Niu, G. Joe, H. Zhao, Y. C. Zhou, T. Orvis, H. X. Huyan, J. Salman, K. Mahalingam, B. Urwin, J. B. Wu, Y. Liu, T. E. Tiwald, S. B. Cronin, B. M. Howe, M. Mecklenburg, R. Haiges, D. J. Singh, H. Wang, M. A. Kats, J. Ravichandran, *Nat. Photonics* **2018**, 12, 392-396; b) L. H. Nicholls, F. J. Rodriguez-Fortuno, M. E. Nasir, R. M. Cordova-Castro, N. Olivier, G. A. Wurtz, A. V. Zayats, *Nat. Photonics* **2017**, *11*, 628-633; c) A. Tagaya, H. Ohkita, M. Mukoh, R. Sakaguchi, Y. Koike, *Science* **2003**, *301*, 812-814.

[2] a) D. Cyranoski, *Nature* **2009**, *457*, 953-956; b) P. S. Halasyamani, K. R. Poeppelmeier, *Chem. Mater.* **1998**, *10*, 2753-2769; c) M. Mutailipu, S. L. Pan, *Angew. Chem. Int. Ed.* **2019**, DOI: 10.1002/ anie.201913974; d) J. Chen, L. Xiong, L. Chen, L. M. Wu, *J. Am. Chem. Soc.* **2018**, *140*, 14082-14086.

[3] a) R. E. Newnham, Properties of materials: anisotropy, symmetry, structure. Oxford University Press on Demand, Oxford, **2005**; b) F. Liang, L. Kang, Z, S. Lin, Y, C. Wu, C. T. Chen, *Coord. Chem. Rev.* **2017**, *333*, 57-70.

[4] a) K. Aoki, H. T. Miyazaki, H. Hirayama, K. Inoshita, T. Baba, K. Sakoda, N. Shinya, Y. Aoyagi, *Nat. Mater.* **2003**, 2, 117-121; b) S. Ghosh, W. H. Wang, F. M. Mendoza, R. C. Myers, X. Li, N. Samarth, A. C. Gossard, D. D. Awschalom, *Nat. Mater.* **2006**, 5, 261-264.

[5] a) W. G. Zhang, H. W. Yu, H. P. Wu, P. S. Halasyamani, *Chem. Mater.* **2017**, *29*, 2655-2668; b) P. Becker, *Adv. Mater.* **1998**, *10*, 979-992; c) J. Chen, C. L. Hu, F. F. Mao, B. P. Yang, X. H. Zhang, J. G. Mao, *Angew. Chem. Int. Ed.* **2019**, *58*, 11666-11669; *Angew. Chem.* **2019**, *131*, 11792-11795.

[6] D. L. Elliott, Ultraviolet laser technology and applications; Academic: Wayland, **2014**.

[7] a) C. T. Chen, N. Ye, J. Lin, J. Jiang, W. R. Zeng, B. C. Wu, *Adv. Mater.* **1999**, *11*, 1071-1078; b) J. J. Zhou, H. P. Wu, H. W. Yu, S. T. Jiang, Z. G. Hu, J. Y. Wang, Y. C. Wu, P. S. Halasyamani, *J. Am. Chem. Soc.* **2020**, *142*, 4616-4620.

[8] a) H. T. Luo, T. Tkaczyk, E. L. Dereniak, K. Oka, R. Sampson, *Opt. Lett.* **2006**, *31*, 616-618; b) G. Ghosh, *Opt. Commun.* **1999**, *163*, 95-102.

[9] a) Y. S. Oseledchik, A. L. Prosvirnin, A. I. Pisarevskiy, V. V. Starshenko, V. V. Osadchuk, S. P. Belokrys, N. V. Svitanko, A. S. Korol, S. A. Krikunov, A. F. Selevich, *Opt. Mater.* **1995**, *4*, 669-674; b) F. Pan, G. Q. Shen, R. J. Wang, X. Q. Wang, D. Z. Shen, *J. Cryst. Growth* **2002**, *241*, 108-114.

[10] a) C. T. Chen, Y. B. Wang, B. C. Wu, K. C. Wu, W. L. Zeng, L. H. Yu, *Nature* **1995**, *373*, 322-324; b) Y. Wang, S. L. Pan, *Coord. Chem. Rev.* **2016**, *323*, 15-35; c) Y. Z. Huang, L. M. Wu, X. T. Wu, L. H. Li, L. Chen, Y. F. Zhang, *J. Am. Chem. Soc.* **2010**, *132*, 12788-12789; d) T. T. Tran, N. Z. Koocher, J. M. Rondinelli, P. S. Halasyamani, *Angew. Chem. Int. Ed.* **2017**, *56*, 2969-2973; *Angew. Chem.* **2017**, *129*, 3015-3019; e) J. L. Song, C. L. Hu, X. Xu, F. Kong, J. G. Mao, *Angew. Chem. Int. Ed.* **2015**, *54*, 3679-3682; *Angew. Chem.* **2015**, *127*, 3750-3753; f) T. T. Tran, J. Young, J. M. Rondinelli, P. S. Halasyamani, *J. Am. Chem. Soc.*, **2017**, *139*, 1285-1295; g) G. H. Zou, N. Ye, L. Huang, X. S. Lin, *J. Am. Chem. Soc.* **2011**, *133*, 20001-20007; h) G. Zou, C. S. Lin, H. Jo, G. Nam, T. S. You, K. M. Ok, *Angew. Chem. Int. Ed.* **2016**, 55, 12078-12082; *Angew. Chem.* **2016**, *128*, 12257-12261; i) S. G. Zhao, Y. Yang, Y. G. Shen, B. Q. Zhao, L. N. Li, C. M. Ji, Z. Y. Wu, D. Q. Yuan, Z. S. Lin, M. C. Hong, J. H. Luo, *Angew. Chem. Int. Ed.* **2017**, *56*, 540-544; *Angew. Chem.* **2017**, *129*, 555-559; j) C. Wu, G. Yang, M. G. Humphrey, C. Zhang, *Coord. Chem. Rev.* **2018**, *375*, 459-488.

[11] a) W. G. Zhang, H. W. Yu, J. Cantwell, H. P. Wu, K. R. Poeppelmeier, P. S. Halasyamani, *Chem. Mater.* **2016**, *28*, 4483-4491; b) J. J. Zhang, Z. H. Zhang, Y. X. Sun, C. Q. Zhang, X. T. Tao, *CrystEngComm* **2011**, *13*, 6985-6990.

[12] a) M. Zhang, D. H. An, C. Hu, X. L. Chen, Z. H. Yang, S. L. Pan, *J. Am. Chem. Soc.* **2019**, *141*, 3258-3264; b) X. L. Chen, B. B. Zhang, F. F. Zhang, Y. Wang, M. Zhang, Z. H. Yang, K. R. Poeppelmeier, S. L. Pan, *J. Am. Chem. Soc.* **2018**, *140*, 16311-16319.

[13] a) M. Luo, F. Liang, Y. X. Song, D. Zhao, F. Xu, N. Ye, Z. S. Lin, *J. Am. Chem. Soc.* **2018**, *140*, 3884-3887; b) X. F. Wang, Y. Wang, B. B. Zhang, F. F. Zhang, Z. H. Yang, S. L. Pan, *Angew. Chem. Int. Ed.* **2017**, *56*, 14119-14123; *Angew. Chem.* **2017**, *129*, 14307-14311; c) M. Mutailipu, M. Zhang, B. B. Zhang, L. Y. Wang, Z. H. Yang, X. Zhou, S. L. Pan, *Angew. Chem. Int. Ed.* **2018**, *57*, 6095-6099; *Angew. Chem.* **2018**, *130*, 6203-6207.

[14] a) Y. C. Liu, X. M. Liu, S. Liu, Q. R. Ding, Y. Q. Li, L. N. Li, S. G. Zhao, Z. S. Lin, J. H. Luo, M. C. Hong, *Angew. Chem. Int. Ed.* **2020**, *59*, 7793-7796; *Angew. Chem.* **2020**, *132*, 7867-7870; b) J. Y. Guo, A. Tudi, S. J. Han, Z. H. Yang, S. L. Pan, *Angew. Chem. Int. Ed.* **2019**, *58*, 17675-17678; *Angew. Chem.* **2019**, *131*, 17839-17842. c) G. Peng, Y. Yang, Y. H. Tang, M. Luo, T. Yan, Y. Q. Zhou, C. S. Lin, Z. S. Lin, N. Ye, *Chem. Commun.* **2017**, *53*, 9398-9401.

[15] a) C. Wu, L. Lin, X. X. Jiang, Z. S. Lin, Z. P. Huang, M. G. Humphrey, P. S. Halasyamani, C. Zhang, *Chem. Mater.* **2019**, *31*, 10100-10108; b) C. Wu, X. X. Jiang, L. Lin, Z. S. Lin, Z. P. Huang, M. G. Humphrey, C. Zhang, *Chem. Mater.* **2020**, *32*, 6906−6915.

[16] F. F. Mao, C. L. Hu, X. Xu, D. Yang, B. P. Yang, J. G. Mao, *Angew. Chem. Int. Ed.* **2017**, *56*, 2151-2155; *Angew. Chem.* **2017**, *129*, 2183-2187

[17] a) L. F. Mei, Y. B. Wang, C. T. Chen, B. C. Wu, *J. Appl. Phys.* **1993**, *74*, 7014-7015; b) S. G. Zhao, P. F. Gong, S. Y. Luo, S. J. Liu, L. N. Li, M. A. Asghar, T. Khan, M. C. Hong, Z. S. Lin, J. H. Luo, *J. Am. Chem. Soc.* **2015**, *137*, 2207-2210.

[18] a) X. H. Dong, L. Huang, Q. Y. Liu, H. M. Zeng, Z. E. Lin, D. G. Xu, G. Zou, *Chem. Commun.* **2018**, *54*, 5792-5795; b) J. R. Thompson, J. S. Ovens, V. E. Williams, D. B. Leznoff, *Chem. Eur. J.* **2013**, *19*, 16572-16578; c) M. Q. Gai, Y. Wang, T. H. Tong, Z. H. Yang, S. L. Pan, *Inorg. Chem.* **2020**, *59*, 4172-4175.

[19] a) G. Q. Zhou, J. Xu, X. D. Chen, H. Y. Zhong, S. T. Wang, K. Xu, P. Z. Deng, F. X. Gan, *J. Cryst. Growth.* **1998**, *191*, 517-519; b) Z. Jia, N. N. Zhang, Y. Y. Ma, L. W. Zhao, M. J. Xia, R. K. Li, *Cryst. Growth Des.* **2017**, *17*, 558-562; c) D. N. Nikogosyan, Nonlinear optical crystals: a complete survey. Springer: **2012**; d) Y. L. Deng, L. Huang, X. H. Dong, L. Wang, K. M. Ok, H. M. Zeng, Z. E. Lin, G. H. Zou, *Angew. Chem. Int. Ed.* **2020**, 10.1002/anie.202009441; e) X. X. Feng, J. J. Zhang, Z. L. Gao, S. J. Zhang, Y. X. Sun, X. T. Tao, *Appl. Phys. Lett.* **2014**, *104*, 081912; f) H. W. Yu, W. G. Zhang, P. S. Halasyamani, *Cryst. Growth Des.* **2016**, *16*, 1081-1087.

[20] a) Y. X. Ma, C. L. Hu, B. X. Li, F. Kong, J. G. Mao, *Inorg. Chem.* **2018**, *57*, 11839-11846; b) F. F. Mao, C. L. Hu, B. X. Li, J. G. Mao, *Inorg. Chem.* **2017**, *56*, 14357-14365; c) S. Lee, H. Jo, K. M. Ok, *J. Solid State Chem.* **2019**, *271*, 298-302; d) G. X. Wang, M. Luo, C. S. Lin, N. Ye, Y. Q. Zhou, W. D. Cheng, *Inorg. Chem.* **2014**, *53*, 12584-12589; e) C. Y. Meng, L. Geng, W. T. Chen, M. F. Wei, K. Dai, H. Y. Lu, W. D. Cheng, *J. Alloys Compd.* **2015**, *640*, 39-44.

[21] W. Kohn, *Rev. Mod. Phys.* **1999**, *71*, 1253-1266.

[22] a) J. Lin, M. H. Lee, Z. P. Liu, C. T. Chen, C. J. Pickard, *Phys. Rev. B* **1999**, *60*, 13380-13389; b) Z. S. Lin, J. Lin, Z. Z. Wang, Y. C. Wu, N. Ye, C. T. Chen, R. K. Li, *J. Phys. Condens. Matter* **2001**, *13*, 369-384.

[23] D. A. Kleinman, *Phys. Rev.* **1962**, *126*, 1977-1979.

[24] R. He, Z. S. Lin, M. H. Lee, C. T. Chen, *J. Appl. Phys.*, **2011**, *109*, 103510.

Entry for the Table of Contents

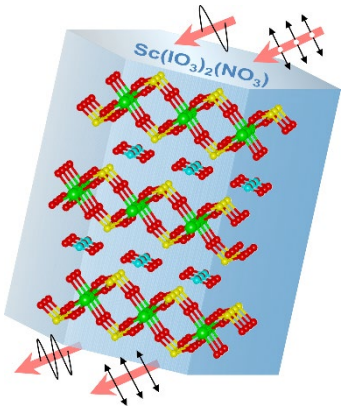

The first 2D rare-earth iodate-nitrate crystal $Sc(IO_3)_2(NO_3)$ (SINO) not only exhibits a strong second-harmonic generation response (4.0 × KH_2PO_4) and short UV absorption edge, but also displays the largest birefringence among inorganic oxide optical crystals thus far (0.348@546 nm).